

Cyclic exchange, isolated states and spinon deconfinement in an XXZ Heisenberg model on the checkerboard lattice

Nic Shannon,¹ Grégoire Misguich,² and Karlo Penc³

¹ *Department of Advanced Materials Science, Graduate School of Frontier Sciences, University of Tokyo, 5-1-5, Kashiwanoha, Kashiwa, Chiba 277-8851, Japan*

² *Service de Physique Théorique, CEA-Saclay, 91191 Gif-sur-Yvette Cédex, France*

³ *Research Institute for Theoretical Solid State Physics and Optics, H-1525 Budapest, P.O.B. 49, Hungary*

(Dated: May 23, 2019)

The antiferromagnetic Ising model on a checkerboard lattice has an ice-like ground state manifold with extensive degeneracy. and, to leading order in J_{xy} , deconfined spinon excitations. We explore the role of cyclic exchange arising at order J_{xy}^2/J_z on the ice states and their associated spinon excitations. By mapping the original problem onto an equivalent quantum six-vertex model, we identify three different phases as a function of the chemical potential for flippable plaquettes — a phase with long range Néel order and confined spinon excitations, a non-magnetic state of resonating square plaquettes, and a quasi-collinear phase with gapped but deconfined spinon excitations. The connection between this quantum six-vertex model and the much studied square-lattice quantum dimer model is also discussed.

PACS numbers: 75.10.-b, 75.10.Jm, 64.60.Cn

The past decade has seen a great renaissance in the study of frustrated quantum spin systems. On the experimental front, advances in the synthesis of magnetic oxides have given rise to a great wealth of new frustrated materials with highly unusual and interesting properties. And, at the same time, highly frustrated models have become a favorite playground of theorists seeking to understand unconventional phase transitions and excitations.

Recently, it was proposed that the geometric frustration present on the pyrochlore lattice could give rise to fractional charges in two or three dimensions,¹ in a physically realistic model based on strong nearest neighbor repulsion close to commensurate filling.² The charge ordering problem considered in¹ is classically equivalent to one of Ising antiferromagnetism, and in this paper we consider the simplest possible test case for these ideas,

the XXZ Heisenberg model on a checkerboard (2D pyrochlore) lattice. We proceed by mapping this model onto an equivalent, *quantum six-vertex model* (Q6VM), and describe the nature of the ground state and low lying spin excitations of this model as a function of a control parameter V , which acts as a chemical potential for those “flippable plaquettes” accessible to cyclic exchange.

We identify three different ground states, a phase with long range Néel order, a non-magnetic state of resonating square plaquettes, and a partially disordered phase of “isolated states” with extremely large ground state degeneracy, referred to as the “quasi-collinear” phase below. Because of the anisotropy of the model, all spin excitations are gapped. In the case of the Néel phase it is possible to identify the lowest lying excitations as spin waves, and in the case of quasi-collinear phase, as deconfined spinons. We also identify the special role of the isolated states in supporting fractional excitations.

Model and mapping onto Q6VM. We take as a starting point the spin-1/2 anisotropic Heisenberg model with antiferromagnetic interactions, $J_z, J_{xy} > 0$, in the limit $J_z \gg J_{xy}$

$$\mathcal{H} = J_z \sum_{\langle ij \rangle} S_i^z S_j^z + \frac{J_{xy}}{2} \sum_{\langle ij \rangle} (S_i^+ S_j^- + S_i^- S_j^+) . \quad (1)$$

Here the sum $\sum_{\langle ij \rangle}$ runs over the bonds of the 2D pyrochlore or checkerboard lattice, shown in Fig. 1a). In the Ising limit, $J_{xy} = 0$, this model has an extensive ground state degeneracy — every state with exactly two up and two down spins per tetrahedron (cross linked square) is a ground state. For historical reasons, this is known as the “ice rules” constraint. Topologically, “ice” states have the structure of closely packed loops of up and down spins. Flipping any given down spin connects two adjacent loops of up spins, creating two “T-junction” like topological defects (spinons), which prop-

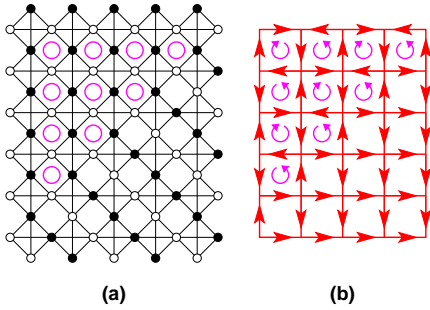


FIG. 1: a) The checkerboard lattice on which the ice states, and b) the square lattice on which the states of the six-vertex model are defined. Any Ising state obeying the ice rules, e.g. that shown in (a), is equivalent to (b) six-vertex model configuration. In the state shown, the upper left corner has Néel order, while the lower right corner has collinear order. Flippable plaquettes are denoted with circles. In the case of the six-vertex model, these have a definite sense of clockwise or anticlockwise rotation

agate independently.^{1,3} The pyrochlore (checkerboard) lattice is bipartite in tetrahedra. Spinons are created in A and B sublattice pairs, and move so as to preserve tetrahedron sublattice.

By drawing an arrow from the center of A to B sublattice tetrahedra where they share an up spin, and from B to A where they share a down spin, one can show that the many ground states of the Ising model on a checkerboard lattice are in exact, one-to-one correspondence with the states of the classical *six vertex model* (6VM),^{4,5,6} widely studied as a 2D analogue of water ice. From this mapping, we know that a) the ground state manifold of the Ising model grows as $W \propto (4/3)^{3N/4}$ where N is the number lattice sites⁷ and b) all correlation functions decay algebraically.⁸

Up to this point, our analysis contains only classical statistical mechanics and simple topological arguments. Quantum mechanics enters the problem when we consider a small but finite $J_{xy} \ll J_z$. Short-lived virtual excitations enable the system to tunnel from one ice state to another wherever pairs of up spins and down spins are found diagonally opposite one another on one of the empty square plaquettes of the checkerboard lattice.⁹ The allowed reconfigurations of these “flippable plaquettes” can be described in perturbation theory by the effective Hamiltonian

$$\mathcal{H}_{\text{2nd}} = -\frac{J_{xy}^2}{J_z} \sum_{\square} (S_1^+ S_2^- S_3^+ S_4^- + S_1^- S_2^+ S_3^- S_4^+), \quad (2)$$

where the indices 1 to 4 count consecutive sites (either clockwise or anticlockwise), of an empty plaquette.⁵ In terms of the 6VM representation, the Hamiltonian (2) acts on a plaquette where four arrow are joined nose to tail, so as to invert all of the arrows and change the sense of rotation of the plaquette (c.f.¹⁰). The quantum dynamics in the Q6VM we consider are directly analogous to the resonance of dimers in the QDM considered by Rokhsar and Kivelson (RK),¹¹ as an simplified model of a short ranged resonating valence bond state.¹² Formally, in fact, the Hamiltonian is exactly the same, although the Hilbert space on which it acts is different. And, as in the

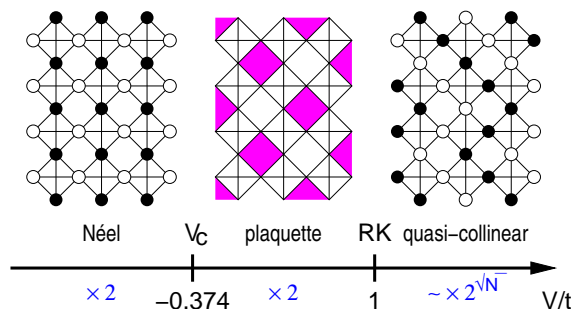


FIG. 2: The phase diagram of the model as a function of V/t . The Néel phase breaks the point group, while the plaquette phase breaks the translational symmetry. The Rokhsar–Kivelson point is marked RK.

QDM, we anticipate that quantum effects will in general select a ground state with finite degeneracy from the vast manifold of classically-allowed ice states.

As such, there is only one (kinetic) energy scale in the problem, $t = J_{xy}^2/J_z$. However in order to study the different possible phases of the model it is useful to introduce a further control parameter. In the case of the classical 6VM this can be done by varying the relative strength of the three pairs of like vertices.⁸ A suitable control parameter for the QDM is a diagonal term which counts the number of dimers which can resonate in any given dimer covering. By direct analogy, we introduce a diagonal interaction V to the Q6VM which counts the number of flippable plaquettes

$$\mathcal{H} = \sum_{\square} [-t(|\circ\rangle\langle\circ| + |\circ\rangle\langle\circ|) + V(|\circ\rangle\langle\circ| + |\circ\rangle\langle\circ|)] \quad (3)$$

where the $|\circ\rangle$ and $|\circ\rangle$ states represent squares with the respective circular arrow configuration on the square edges, as seen in Fig. 1(b).

Our approach to determine the different phases of the Hamiltonian (3) is the numerical diagonalization of clusters of up to 64 spins, within the ice rules manifold of states, supplemented with topological and symmetry arguments. Details of these, together with further analysis of the related fermionic charge-ordering problem will be discussed further in separate publications.^{13,14}

Phase diagram We first consider the nature of the ground state as a function the chemical potential for flippable plaquettes, V . Our results are summarized in the phase diagram Fig. 2, and the numerical evidence for each phase discussed below.

Negative values of V favor states with flippable plaquettes. The state with the greatest possible number of flippable plaquettes is the Néel state, and this must be the ground state for $V \rightarrow -\infty$. The Néel state is two fold degenerate in the thermodynamic limit. For finite V/t , in a finite size system, quantum fluctuations lift this degeneracy.

The low lying states of the Q6VM we consider are shown in Fig. 3. We find a single phase for $V \lesssim -0.3t$, which we identify as the Néel phase. Both the the symmetric and antisymmetric combinations of the two symmetry-breaking Néel ground states are visible in the spectrum, marked “GS” and “ $\overline{Néel}$ ” respectively. At a value of $V/t \sim 0.3$, a third energy level, marked “ \overline{Plaq} ” crosses the first excitation “ $\overline{Néel}$ ”. We interpret this as evidence for a quantum phase transition into a resonating plaquette phase, discussed below. From finite size scaling of the spectrum (Fig. 4) we estimate the critical value to be $V/t = -0.3727$ in the thermodynamic limit. As the competing Néel and plaquette order parameters break lattice symmetries in very different ways, the transition between them is presumably of first order.

We find a single phase extending from $-0.3t \lesssim V \leq t$, including the XXZ point $V = 0$. This phase terminates in the special high symmetry point $V = t$ for which the

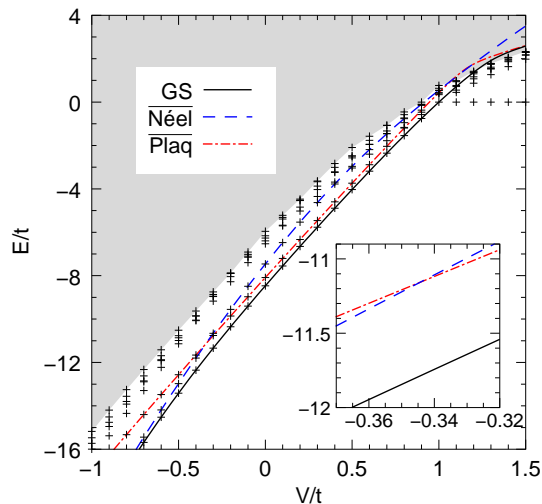


FIG. 3: Energy level diagram of the 32-site pyrochlore-slab with periodic boundary conditions as a function of V/t , obtained by numerical diagonalization. We have shown the first 8 levels. Inset: the first two excited states cross at $V_c/t = -0.3437$ (the axes are the same as of the main plot).

Hamiltonian (3) of the Q6VM can be written in the form of a projection operator :

$$\mathcal{H}_{\text{RK}} = t \sum_{\square} (|\odot\rangle - |\circ\rangle)(\langle\odot| - \langle\circ|). \quad (4)$$

Following Rokhsar and Kivelson, we can construct a zero eigenvalue of the Hamiltonian (4) by taking the linear combination of all the states in a given topological sector with the same amplitude, i.e.

$$|\text{RK}\rangle = \mathcal{P}_{6V} \prod_{\square} (|\odot\rangle + |\circ\rangle) \quad (5)$$

where the product \prod_{\square} runs over empty plaquettes and the operator \mathcal{P}_{6V} projects onto states permitted by the ice rules. Since this state is annihilated by the Hamiltonian Eq. 4, which is positive semi-definite, it must be a ground state. As in the QDM, static correlations can be computed exactly at this point. Like the correlation functions of the 6VM, they decay algebraically with distance.

At the RK point, kinetic and potential energy are perfectly balanced; in the plaquette phase kinetic energy dominates, and resonating plaquettes repel one another so as gain the maximum kinetic energy. The resulting state is essentially a Peierls-like distortion of the RK state in which only A (B) sublattice plaquettes resonate $\prod_{\square_{A(B)}} (|\odot\rangle + |\circ\rangle)$. The way in which the phase breaks lattice symmetries — it is two-fold degenerate, and invariant under operations which map the alternating A and B plaquette sublattice onto themselves — suggest the plaquette phase of the Q6VM is an Ising analogue of the a SU(2) valence-bond crystal of resonating plaquettes.¹⁵ Such a phase has been proposed in the context of the

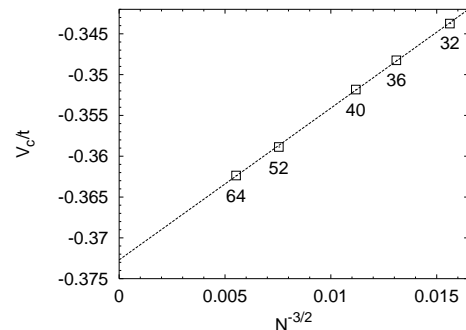


FIG. 4: Estimate of the phase boundary between the Néel and plaquette phases. Empirically, the values of V_c where the level crossings occur scale as $-0.3727 + 1.86N^{-3/2}$. Values are shown for 32, 36, 40, 52, and 64 pyrochlore-slab sites.

square lattice QDM.¹⁶ Furthermore, extensive numerical calculations have shown that the ground state of the Heisenberg-model on a checkerboard lattice is a valence bond crystal of SU(2) singlets formed on alternate empty plaquettes (see¹⁷ and references therein). We are therefore tempted to speculate that there may be an adiabatic continuity between the ground state of the XXZ and SU(2) symmetric Heisenberg models on the checkerboard lattice.¹⁸

The phase found for $V > t$ can most easily be understood by considering the limit $V/t \rightarrow \infty$. In this case the ground state is the highly degenerate manifold of “isolated” state with no flippable plaquettes. More precisely, they are also eigenstates with 0 energy for any value of V/t , and become the ground state for $V > t$. The prototype of an isolated state is the collinear configuration shown in Fig 1. In this reference state all vertex arrows point from left to right or from top to bottom. Inverting the direction of the arrows along a given horizontal (or vertical) line creates a new state within the ground state manifold. We can invert the direction of the arrows on an arbitrary number of lines, subject to the constraint that all of them are either horizontal or vertical. This leads to a ground state degeneracy which grows as $4(2^p - 1)$ for regularly shaped clusters, where $p \sim \sqrt{N}$. In these states, the direction of arrows along either the horizontal or vertical lines is long-range ordered. The Ising-like form of degeneracy has important implications for its excitations, discussed below.

We refer to this phase of the Q6VM as quasi-collinear. It can naively be viewed as being “disordered” in the sense that quantum effects fail to select a ground state with finite degeneracy. However, in this sense, the ice manifold of ground states of the Ising model on the checkerboard lattice is also disordered, and the correlation functions of the 6VM at the ice point are known to show algebraic rather than exponential decay.⁸ And within the isolate state manifold, simply fixing the spins at the boundary of a cluster is enough to select a unique ground state. We note that in the “super-frustrated”

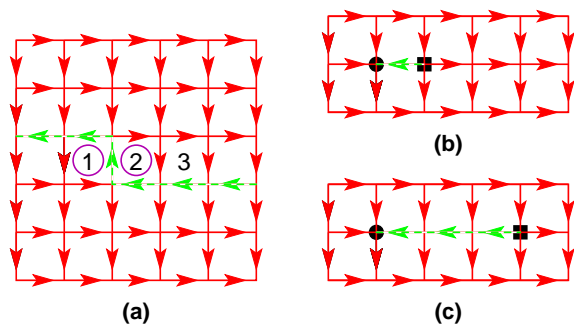


FIG. 5: (a) A “leap-frog” excitation in the quasi-collinear phase. Two flippable plaquettes (denoted with circles) are created by reversing the arrows of the collinear reference state on a line with a single one-step kink. The motion of the pair of flippable plaquettes is equivalent to a one-dimensional hopping model with an energy spectrum $\varepsilon(k) = 2V + 2t \cos k$, where k is an effective one-dimensional momentum. (b) and (c): In the collinear phase spinon excitations (black dots), can deconfine as there is no string potential associated with their separation. Note that spinons hop so as to stay within a given sublattice of the (bi-partite) square lattice.

case of the the Kagome lattice, where no isolated states exist, correlation functions decay exponentially.¹⁹ Finally, since the transition between the quasi-collinear phase and the resonating plaquette phase takes place through the softening of specific excitation (discussed below), we identify it as second order.

Excitations. First let us first consider the nature of excitations at fixed $S^z = 0$. A state with n flippable plaquettes has a diagonal matrix element nV and is connected to n other states. Gerschgorin’s theorem places a bound $|H_{ii} - \varepsilon_i| < \sum_j |H_{ij}|$ on the separation of the i -th eigenvalue ε_i from the diagonal matrix element H_{ii} . In the case in point, this bound is $|nV - \varepsilon_i| < nt$, or $n(V - t) < \varepsilon_i < n(V + t)$. The smallest energy in an arbitrary topological sector is thus larger than $V - t$, which gives a lower bound on the value of the gap in the quasi-collinear phase for $V > t$. This above argument permits a gapless spectrum at the Rokhsar-Kivelson point ($V = t$). In fact it is possible to explicitly construct a family of states with gapless excitations at the RK point, and which energy saturates the lower bound for $V > t$. An example is shown in Fig. 5(a). As the energy spectrum of this particular excitation form a continuum between $2V - 2t$ and $2V + 2t$, with a gap that vanishes at the RK point. We note that this excitation can also be constructed for the equivalent phase of the QDM.

Now let us consider what happens to spin excitations.

If we neglect virtual processes at order J_{xy}^2/J_z , these propagate as independent fractional excitations.¹ Quantum effects may, or may not, act to confine these excitations, depending on the type of correlations present in the the ground state they select. The Néel ground state has a finite (two fold) ground state degeneracy, and separating the topological defects created by flipping a spin creates a string of unflippable plaquettes. This leads to a linear string confinement of spinons, and the low lying spin excitations of the Néel phase of our model have the same quantum numbers as a spin wave. On general grounds, we expect the same to true of the resonating plaquette phase.

The manifold of isolated states selected by V can support deconfined spinons, however. Since no new flippable plaquettes are introduced into isolated states by flipping a single spin, and the pair of topological defects created by flipping a single spin can be separated without creating new flippable plaquettes, spinons are deconfined. An example of a pair of deconfined spinon excitations, with gap $J_z - 2J_{xy}$ and bandwidth $4J_{xy}$ is shown in Fig. 5(b)-(c). While their movement is confined to the x and y directions, by scattering off one another, the pair of spinons can explore the full two dimensional space of the checkerboard lattice. We note that an equivalent zero-energy line defect can also be constructed in the corresponding phase of the square-lattice QDM.

Conclusions We have established that, as a function of the chemical potential for “flippable plaquettes” accessible to cyclic exchange, the XXZ Heisenberg model on a checkerboard lattice exhibits Néel, resonating plaquette and quasi-collinear phases. If virtual processes at J_{xy}^2/J_z are ignored, spinon excitations in the XXZ Heisenberg model are deconfined. We have shown explicitly that a subset of spinon excitations — those associated with isolated states — remain deconfined even when these quantum effects are taken into account. These are the low-lying spin excitations of the quasi-collinear phase of the model. This analysis is also relevant to the QDM on a square lattice,²⁰ and to the class of statistical mechanics problems which are classically equivalent to the 6VM.

Acknowledgements We are pleased to acknowledge helpful discussions with P. Fazekas, P. Fulde, R. Moessner, V. Pasquier, E. Runge, D. Serban, A. Sütő, M. Roger, P. Sindzingre and P. Wiegmann. K. P. was supported by the Hungarian OTKA T038162 and T037451, N.S. was supported by EU RTN “He III Neutrons”. Both K.P. and N.S. have enjoyed the hospitality of the guest program of MPI-PKS Dresden.

¹ P. Fulde, K. Penc and N. Shannon, Ann. Phys. (Leipzig) **11**, 892 (2002).

² P. W. Anderson, Phys. Rev. **102**, 1008 (1956).

³ M. Hermele and M. P. A. Fisher and L. Balents, Phys.

Rev. B **69**, 064404 (2004).

⁴ J. Kohanoff, G. Jug, and E Tosatti, J. Phys. A **23**, L209 (1990)

⁵ R. Moessner, O. Tchernyshyov and S. L. Sondhi,

cond-mat/0106286.

- ⁶ R. Moessner and S. L. Sondhi, Phys. Rev. B **63**, 224401 (2001).
- ⁷ E. Lieb, Phys. Rev. Lett. **18**, 692 (1967).
- ⁸ R. Baxter, *Exactly Solved Models in Statistical Mechanics*, (Academic Press, San Diego, 1982), pages 127-179.
- ⁹ This is in marked contrast to the XXZ model on a triangular lattice, where the states in the ground-state manifold are connected directly by J_{xy} , leading to the RVB picture in P. Fazekas and P. W. Anderson, Philos. Mag. **30**, 423 (1974).
- ¹⁰ S. Chakravarty, Phys. Rev. B **66**, 224505 (2002).
- ¹¹ D. S. Rokhsar and S. A. Kivelson, Phys. Rev. Lett. **61**, 2376 (1988).
- ¹² P. W. Anderson, Mater. Res. Bull. **8**, 153 (1973).
- ¹³ K. Penc and N. Shannon, in preparation.
- ¹⁴ E. Runge and P. Fulde, submitted to Phys. Rev. B.
- ¹⁵ The plaquette phase is also recently been observed in Quantum Monte Carlo simulations. (R. Moessner, private communication.)
- ¹⁶ P. W. Leung and K. C. Chiu and K. J. Runge, Phys. Rev. B **54**, 12938 (1996).
- ¹⁷ P. Sindzingre, J.-B. Fouet and C. Lhuillier, Phys. Rev. B **66**, 174424, (2002).
- ¹⁸ Further numerical work confirms this conjecture (P. Sindzingre, private communication).
- ¹⁹ A. Sütő, Z. Phys. B **44**, 121 (1981)
- ²⁰ The similarity between the two models can be traced back to the lattice bipartiteness and the existence of a common height representation for both the dimer coverings (H. W. J. Blote and H. J. Hilhorst, J. Phys. A **15**, L631 (1982)) and 6VM states⁶, where isolated states are those with a maximum "tilt".